Few-Body Syst (2016) 57:331–336
DOI 10.1007/s00601-016-1082-4

A. Bonaccorso · F. Carstoiu · R. J. Charity · R. Kumar
G. Salvioni

Differences Between a Single- and a Double-Folding Nucleus-^{9}Be Optical Potential

Received: 30 December 2015 / Accepted: 4 March 2016 / Published online: 22 March 2016

Abstract We have recently constructed two very successful n-^{9}Be optical potentials (Bonaccorso and Charity in Phys Rev C89:024619, 2014). One by the Dispersive Optical Model (DOM) method and the other (AB) fully phenomenological. The two potentials have strong surface terms in common for both the real and the imaginary parts. This feature makes them particularly suitable to build a single-folded (light-) nucleus-^{9}Be optical potential by using ab-initio projectile densities such as those obtained with the VMC method (Wiringa http://www.phy.anl.gov/theory/research/density/). On the other hand, a VMC density together with experimental nucleon–nucleon cross-sections can be used also to obtain a neutron and/or proton-^{9}Be imaginary folding potential. We will use here an ab-initio VMC density (Wiringa http://www.phy.anl.gov/theory/research/density/) to obtain both a n-^{9}Be single-folded potential and a nucleus-nucleus double-folded potential. In this work we report on the cases of ^{8}B, ^{8}Li and ^{8}C projectiles. Our approach could be the basis for a systematic study of optical potentials for light exotic nuclei scattering on such light targets. Some of the projectiles studied are *cores* of other exotic nuclei for which neutron knockout has been used to extract spectroscopic information. For those cases, our study will serve to make a quantitative assessment of the core-target part of the reaction description, in particular its localization.

The work of R.J. Charity was supported by the U.S. Department of Energy, Office of Science, Office of Nuclear Physics under Award No. DE-FG02-87ER-4036.

A. Bonaccorso (✉)
INFN, Sez. di Pisa, Largo B. Pontecorvo 3, 56127 Pisa, Italy
E-mail: bonac@df.unipi.it

F. Carstoiu
Institute of Atomic Physics, P.O. Box MG-6, Bucharest, Romania

R. J. Charity
Department of Chemistry, Washington University, St. Louis, MO 63130, USA

R. Kumar
Department of Physics, Deenbandhu Chhoturam University of Science and Technology, Murthal, Sonepat, Haryana 131039, India

G. Salvioni
Dipartimento di Fisica, Università di Pisa, Largo B. Pontecorvo 3, 56127 Pisa, Italy

Present address
G. Salvioni
Department of Physics, University of Jyvaskyla, P.O. Box 35 (YFL), FI-40014 Jyvaskyla, Finland

1 Introduction

Light exotic nuclei have been studied extensively in the last thirty years and their structure was first enlightened from measurements of the total reaction cross sections analyzed in terms of the Glauber model [1]. This lead automatically to calculations of imaginary parts of the nucleus-nucleus optical potential in the folding model. Such a procedure, although very simple, is questionable because the folding model is first order in the nucleon-nucleon interaction, while the Feshbach imaginary potential is second order for a real nucleon-nucleon interaction. Furthermore for light projectiles on light targets the optical model itself has to be handled with great care.

In the following we will present simple ideas to overcome the above difficulties. First we will show that an "all order" potential can be obtained if, instead of using a double folding model, one uses a single folding model in which a microscopic projectile density is folded with a phenomenological n-target optical potential and explicit breakup channels of the projectile can be introduced via a small additional surface term.

The potentials thus obtained will be used to calculate S-matrices and total reaction cross sections for the systems ^{8}Li-^{9}Be and ^{8}B-^{9}Be for which experimental data exist. The comparison between our model calculations and the data will show that the procedure leads to encouraging results which could have interesting applications in knockout formalisms as well.

2 Nucleus-Nucleus Optical Potential

In the Glauber description of nucleus-nucleus scattering the reaction cross section is given by

$$\sigma_R = \int_0^\infty d\mathbf{b}\left(1 - |S_{NN}(\mathbf{b})|^2\right) \tag{1}$$

where

$$|S_{NN}(\mathbf{b})|^2 = e^{2\chi_I(b)} \tag{2}$$

can be interpreted as the probability that the scattering is elastic for a given impact parameter.

At low energy, it is important to take into account the Coulomb deflection. In this case, the impact parameter can be substituted by the distance of closest approach in the S-matrix calculation b$\rightarrow b' = a_c + \sqrt{a_c^2 + b^2}$, with a$_c$ the Coulomb-length parameter.

The imaginary part of the eikonal phase shift can be written as

$$\begin{aligned}\chi_I(\mathbf{b}) &= \frac{1}{\hbar v}\int dz\; W^{NN}(\mathbf{b}, z)\\ &= \frac{1}{\hbar v}\int dz \int d\mathbf{b_1}\; W^{nN}(\mathbf{b_1} - \mathbf{b}, z)\int dz_1\; \rho(\mathbf{b_1}, z_1)\end{aligned} \tag{3}$$

where W^{NN} is negative defined and

$$W^{NN}(\mathbf{r}) = \int d\mathbf{r_1} W^{nN}(\mathbf{r_1} - \mathbf{r})\rho(\mathbf{r_1}) \tag{4}$$

is the imaginary part of the single-folded optical potential given in terms of the nucleon-nucleus optical potential $W^{nN}(\mathbf{r})$ and the matter density $\rho(\mathbf{b_1}, z_1)$ of the other nucleus. In the single-folding method $W^{nN}(\mathbf{r})$ can be the imaginary part of a phenomenological nucleon-target potential such as the (DOM) or the (AB) potentials of Ref. [2]. However, W^{NN} can also be obtained from the double-folding method using microscopic densities $\rho_{p,t}(\mathbf{r})$ for the projectile and target respectively and an energy dependent nucleon-nucleon cross section σ_{nn}, i.e,

$$W^{NN}(\mathbf{r}) = -\frac{1}{2}\hbar v\sigma_{nn}\int d\mathbf{b_1}\; \rho_p(\mathbf{b_1} - \mathbf{b}, z)\int dz_1\; \rho_t(\mathbf{b_1}, z_1). \tag{5}$$

Here

$$W^{nN}(\mathbf{r}) = -\frac{1}{2}\hbar v\sigma_{nn}\rho_t(\mathbf{r}). \tag{6}$$

would be a single-folded zero-range n-target imaginary potential and v is the nucleon-target velocity of relative motion. This equation shows that the W^{nN} potential has the same range as the target density because σ_{nn} is a simple scaling factor and does not contain much dynamical effects.

In this case, the phase shift becomes:

$$\chi_I(\mathbf{b}) = -\frac{1}{2}\sigma_{nn}\int d\mathbf{b_1}\int dz\ \rho(\mathbf{b_1}-\mathbf{b},z)\int dz_1\ \rho(\mathbf{b_1},z_1). \tag{7}$$

A finite range potential can also be defined as:

$$W^{NN}(\mathbf{r}) = -\frac{1}{2}\hbar v\int d\mathbf{r_1}d\mathbf{r_2}\ \rho_p(\mathbf{r_1})\ \rho_t(\mathbf{r_2})v_{nn}(\mathbf{r_1}+\mathbf{r}-\mathbf{r_2}) \tag{8}$$

Where v_{nn} can be a finite-range or zero-range Gogny or M3Y or phenomenological nucleon-nucleon interaction. Equation (8) can give reasonable potentials whose imaginary parts need however to be renormalized most of the times.

In this paper we will: (i) first compare the characteristics of the imaginary potentials from Ref. [2] with those of the potential obtained from Eq. (6) with the ^{9}Be density from Ref. [3]; (ii) calculate Eq. (3) with the potentials of Ref. [2] and Eq. (5) with the microscopic densities; (iii) compare the respective S-matrices from Eq. (2) and obtain the strong absorption radii R_s defined as $|S_{NN}(R_s)|^2 = \frac{1}{2}$; (iv) calculate the reaction cross sections obtained from Eq. (1).

3 n-^{9}Be Imaginary Potential

In this section we compare the (DOM) and (AB) potentials with the potential from Eq. (6). Figure 1 shows on the LHS, the neutron-^{9}Be imaginary potential at 100 MeV. The blue full curve, is the (AB) potential from Ref. [2] while the dotted curves are from Eq. (6) using ^{9}Be density from Ref. [3,4]. The red curve was obtained using σ_{np} while the blue curve with σ_{pp} for which we used the parametrized form given in Ref. [5]. The RHS is the same as the LHS but at an energy of 40 MeV. The red full curve is the (DOM) potential from Ref. [2]. This figure shows that both "phenomenological" potentials (DOM) and (AB) are dominated by surface components and have a longer range than the folded potential, although the latter is obtained from a realistic density. For example at 40 MeV we get $< r^2 >^{1/2} = 2.72$ fm for the (AB) potential and $< r^2 >^{1/2} = 3.12$ fm for the (DOM) potential while the folded potential gives $< r^2 >^{1/2} = 2.41$ fm. Notice also that the ^{9}Be density from Ref. [3] provides $< r^2 >^{1/2} = 2.42$ fm while the charge distribution r.m.s. from Ref. [6] is 2.519 fm. Thus it is clear that a folded potential is affected by the ambiguities discussed in Ref. [7] related to the choice of the nucleon-nucleon cross section, but what is most important at least for a light, very deformed nucleus like ^{9}Be, it will miss the strong dynamical effect, contained instead in a phenomenological potential, of a surface dominance and a longer range.

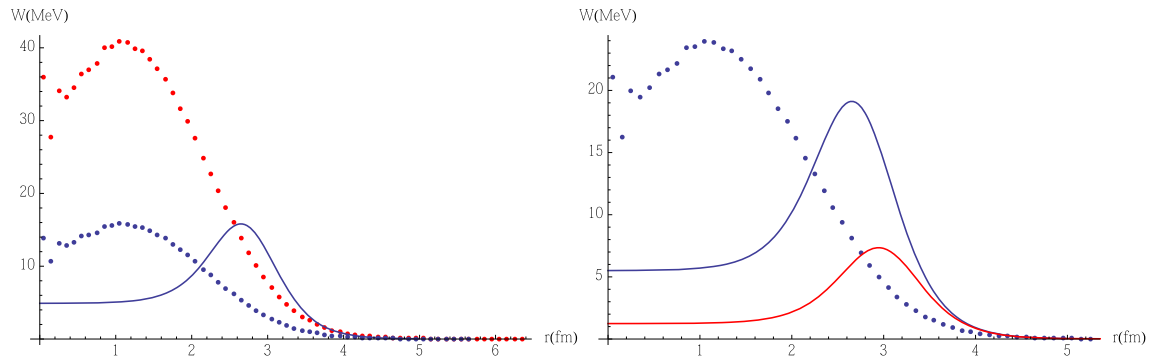

Fig. 1 (*Color online*) LHS: Absolute values of neutron-^{9}Be imaginary potential at 100 MeV. *Blue full curve*, (AB) potential from Ref. [2]. *Dotted curves* from Eq. (6) using ^{9}Be density from Ref. [3]. *Red* with σ_{np}, *blue* with σ_{pp}. RHS: Same as LHS but at 40 MeV. The *red full curve* is the (DOM) potential from Ref. [2]

4 Nucleus-^{9}Be Imaginary Potential

In this section we discuss nucleus-nucleus imaginary potentials for scattering of light exotic nuclei on a ^{9}Be target. Already in the seminal paper by Satchler and Love [8] on the folding model for ^{9}Be scattering, the authors found evidence of anomalously large deformation and surface effects, which is consistent with the results of [2]. However one characteristic of a folded potential is that its radial shape is determined solely by those of the densities used. As such the distinction of surface and volume terms and in particular their respective contribution, which is strongly energy dependent, as shown by phenomenological potentials, cannot be reproduced. Indeed when experimental data are available, this problem is often solved by renormalizing the folded potential so that it would reproduce the data. But dynamical aspects of surface reactions which are typical and very relevant for light nuclei would be difficult to reproduce by a folded potential which then cannot have any predictive power. We will show in the following that a better way to determine the imaginary part of a nucleus-nucleus potential for light exotic ions is to make a single folding calculation using one density and one nucleon-nucleus phenomenological potential, provided the latter is available from a fit to experimental data. The accuracy of such a procedure can be checked by using the potentials to calculate total reaction cross sections, whose experimental values are now available in many cases. Such cross sections will be reproduced, in the eikonal approximation, without renormalizing the potential at energies larger than about 80 A.MeV [9]. Thus it appears that the energy dependence of the n-nucleus potential is enough to provide the correct energy dependence of the nucleus-nucleus potential, which will then have an accurate predictive power.

We will study a series of potentials and calculate the reaction cross sections obtained by using them, for scattering of light exotic nuclei on a ^{9}Be target. The double folding will be calculated by using VMC densities. Calculations with HF densities, and the JLM method will be presented elsewhere [9]. On the other hand we will fold the (DOM) and (AB) potentials of Ref. [2] with the same VMC densities used in the double folding and compare the results. This procedure will suggest ways to determine the "strong absorption radius" for the core-target elastic scattering in one-nucleon knockout reactions and thus to constraint the core-target S-matrix S_{ct} which is a very relevant quantity in the calculation of the absolute cross sections and in the extraction of the "experimental" spectroscopic factors.

First we show in Fig. 2, (LHS), the ^{8}B-^{9}Be cases at 65AMeV. The starting points are the n-^{9}Be potentials shown in the RHS of Fig. 1 and the ^{8}B density from Ref. [3,4]. The full blue and red dot-dashed curves are obtained with the (AB) and (DOM) potentials respectively while the green curve is obtained from the double-folded potential, Eq. (5), where σ_{pp} was used. The corresponding r.m.s. radii are $< r^2 >^{1/2} = 3.66$, 3.87, 3.36 fm. On the other hand the r.m.s. of the total densities used are $< r^2 >^{1/2} = 2.34$, 2.66 fm for ^{8}B and ^{8}C respectively. On the (RHS) we show the corresponding impact parameter dependence of $|S_{NN}|^2$ which have R_s = 5.38, 5.14 and 4.8 fm respectively according to the following parametrization:

$$S_{NN} = \exp\left(-\ln 2 \exp((R_s - b)/a)\right) \tag{9}$$

with a diffuseness like parameter a = 0.65 fm, and R_s the strong absorption radius.

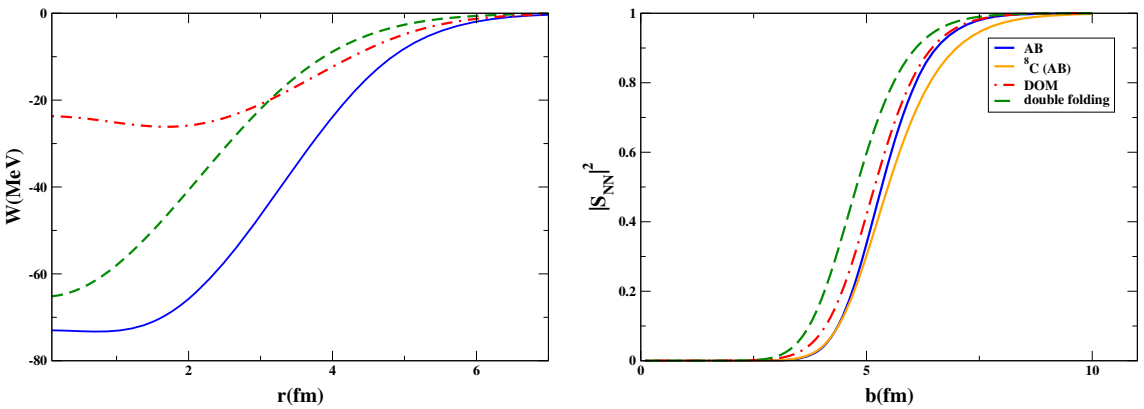

Fig. 2 (*Color online*) LHS: ^{8}B-^{9}Be folding potentials. Obtained with ^{8}B density from Ref. [3]. The *blue full curve* and *red dot-dashed curve* are obtained with the (AB) and (DOM) potentials respectively for n-^{9}Be while the *green dashed curve* is the double-folded potential, Eq. (5) where σ_{pp} was used. RHS: $|S_{NN}|^2$ corresponding to the potentials on the LHS. The *orange full curve* is for a '^{8}C' projectile

Table 1 Energy dependent strong absorption radii and calculated total reaction cross sections compared to experimental values from Refs. [10,11] for ^{8}Li+^{9}Be and ^{8}B+^{8}Be

E_{lab} (AMeV)	$\sigma_{exp}(^{8}\mathrm{Li})$ (mb)	σ_{th} (mb)	E_{lab} (AMeV)	$\sigma_{exp}(^{8}\mathrm{B})$ (mb)	σ_{th} (mb)	R_s (fm)	r_s (fm)
40.9	1124 ± 15	990–1132	37.5	1306 ± 13	996–1281	5.55	1.36
60.9	1002 ± 15	930–1011	60.2	1087 ± 24	935–1096	5.35	1.31
86.3	856 ± 17	869				5.20	1.27
96.8	816 ± 14	847				5.05	1.24
105.4	781 ± 13	829				4.95	1.21

The upper values (RHS) in the two columns σ_{th} are obtained with a surface correction to the folded potential

Due to the energy dependence of the optical potential, the strong absorption radius is also energy dependent. It is customary to parametrize such as a dependence as

$$R_s = r_s(E_{inc}) \left(A_p^{1/3} + A_t^{1/3} \right). \tag{10}$$

It is interesting to see that although the potentials on the (LHS) of Fig. 2 are evidently very different, their r.m.s. radii are quite close to each other. However the corresponding strong absorption radii are very different from each other and would give large differences in the absolute knockout cross section.

The orange curve on the (RHS) of Fig. 2 is for a '^{8}C' projectile. It can be parametrized according to Eq. (9) with $R_s = 5.45$ fm and $a = 0.85$ fm. It is interesting to see in this case how the large values of the parameters of the S-matrix reflect the "unbound" nature of ^{8}C and thus the extreme peripheral nature of the reactions involving it.

It is useful to compare our results with existing experimental data from Refs. [10,11] in which reaction cross sections for ^{8}B-^{9}Be and ^{8}Li-^{9}Be have been measured and density distributions have been extracted using a Glauber model. These data point out to a different density distribution for ^{8}B and ^{8}Li in contrast to the expectation from isospin symmetry that they should be the same. Our calculated values are given in Table 1 and they are in very good agreement with both the absolute values of the experimental cross sections and their energy dependence at all but the two lowest energies. We notice that at such energies the loosely bound nature of the projectiles would provide a Dynamical Polarization Potential representing the valence nucleon breakup channel. Since the folding model misses such a term, we have added a surface potential with very small strength (0.6 and 0.4 MeV for ^{8}B and 0.3 and 0.2 MeV for ^{8}Li), the radius has been taken equal to 3.7 fm in both cases while the diffuseness has been taken large, following the prescription of [12] and equal to $1/(2\sqrt{2mS_{p,n}}/\hbar)$ which gives 2.95 and 1.6 fm respectively for ^{8}B and ^{8}Li. In this way we have obtained the cross sections given as the upper values (and RHS) in the columns σ_{th}. The agreement with the experimental cross sections is now quite amazing and it suggests that this would be an interesting way to consider for further improvements to the folding model.

5 Conclusions

In this short contribution we have presented some preliminary results obtained using new ideas to improve the calculation of the nucleus-nucleus imaginary potential, the corresponding S-matrices and total reaction cross sections. We have been concerned concerned with light exotic nuclei for which the optical model and, in particular, the folding-model version of it needs careful handling and a good understanding of the reaction channels involved. We have improved the existing formalisms by using a single folding model in which the n-^{9}Be target potential has been taken from a phenomenological fit to data over a large range of energies [2]. Projectile densities have been taken from very accurate microscopic ab-initio calculations [3]. Finally when necessary, we have introduced a semi-microscopic surface term according to [12]. The results are extremely encouraging and a full systematic study along these lines is in progress.

References

1. Tanihata, I.: Neutron Halo Nuclei. J. Phys. G Nucl. Part. Phys. **22**, 157 (1996)

2. Bonaccorso, A., Charity, R.J.: Optical potential for the n-9Be reaction. Phys. Rev. C **89**, 024619 (2014)
3. Wiringa, R.B.: http://www.phy.anl.gov/theory/research/density/
4. Pieper, S.C., Wiringa, R.B.: Quantum Monte Carlo Calculations of Light Nuclei. Annu. Rev. Nucl. Part. Sci. **51**, 53 (2001)
5. Xiangzhou, C., Jun, F., Wenqing, S., Yugang, M., Jiansong, W., Wei, Y.: In-medium nucleon-nucleon cross section and its effect on total nuclear reaction cross section. Phys. Rev. C **58**, 572 (1998)
6. De Vries, H., De Jager, C.W., De Vries, C.: Nuclear charge-density-distribution parameters from elastic electron scattering. At. Data Nucl. Data Tables **36**, 495–536 (1987)
7. Bertulani, C.A., De Conti, C.: Pauli blocking and medium effects in nucleon knockout reactions. Phys. Rev. C **81**, 064603 (2010)
8. Satchler, G.R., Love, W.G.: Folding model potentials from realistic interactions for heavy-ion scattering. Phys. Rep. **55**, 183 (1979)
9. Bonaccorso et al., A.: (in preparation)
10. Fan, G.W., et al.: Structure of Li8 from a reaction cross-section measurement. Phys. Rev. C **90**, 044321 (2014)
11. Fukuda, M., et al.: Density distribution of 8B studied via reaction cross sections. Nucl. Phys. A **656**, 209 (1999)
12. Bonaccorso, A., Carstoiu, F.: Optical potentials of halo and weakly bound nuclei. Nucl. Phys. A **706**, 322 (2002)